

## ALTERNATIVE METHODS FOR MULTIPLE LASER BEAMS GENERATION

Laura IONEL<sup>1,2</sup>

*The importance of simultaneous optical monitoring of many objects or several zones of the same object was already established. This paper reports two alternative methods for multiple laser beam generation using diffractive masks and phase modulation. They use linear blazed gratings combination LBGC or as quasi-periodic structures QPSs with parameters chosen in accordance with the desired multi-spots features. After masks are displayed on a spatial light modulator, the corresponding experimental diffraction patterns are analyzed in terms of diffracted intensity to show the advantages of each method. A code including sparse template was developed to obtain spots focused in different planes perpendicular to the optical axis. The theoretical aspects of the diffractive masks design, experimental configuration and results are presented and discussed.*

**Keywords:** Spatial light modulator, Diffractive optics, Multiple laser beams, Blazed gratings, Iterative Fourier transform algorithm.

### 1. Introduction

Lately, significant research has demonstrated the importance of the phase masks presence in various applications such as: lithography, optical tools for security, sensors or solar cells [1-4]. Also, diffractive gratings proved during the last decades to play a very important role for speckle contrast reduction in laser projector or structured beams generators in association with specific opto-electronic elements (e.g. spatial light modulators (SLM) [5] or diffractive optical elements [6,7]). Moreover, the blazed diffraction gratings are widely used as the optimal shape design for mask-etch fabrication due to its basic property to steer the light in a given direction [8].

In this work, we propose and compare two alternative methods to obtain multiple laser beams with the aim of being directed to illuminate different objects or different zones from the same object. The first is a flexible and versatile method using diffractive masks which consists in a predefined number of blazed gratings arranged in a specific configuration and addressed on a spatial light modulator. The second is a method based on quasi-periodic structures, studied in terms of multiple beam features such as: the distance to the optical axis,  $R$ , spots radius,  $r$ , diffraction efficiency or focus plane; they are also addressed on SLM as diffractive phase masks. In the last years, SLMs have been successfully

<sup>1</sup> Researcher, Phys. Dept., POLITEHNICA University of Bucharest, Romania

<sup>2</sup> Researcher, National Institute for Laser, Plasma and Radiation Physics, Romania, e-mail: laura.ionel@inflpr.ro

implemented in a wide variety of applications, such as: micro and nano-processing [9,10], triple beams configuration [11] holographic optical tweezers [12,13], temporal and spatial beam shaping [14,15], surface topology measurements and reconstruction [16] or wave front correction [17]. In the present paper, a spatial light modulator has been used both as a beam splitter for the multiple laser beam generation employing diffractive masks and as a beam steering device which offers a precise control of the angle between the generated beams. In the last decade, the multiple beam concept plays a very important role in a wide range of applications such as: x-ray laser generation [18], multiple THz pulse generation [19], satellite communication [20], laser interferometry [21] or multibeam lithography [22]. The methods presented here have been designed to offer accurate and variable multi-spot patterning with high resolution for various applications such as optical monitoring, sensing, ultra-short pulse laser processing or photonic crystals generation [23, 24].

## 2. Multiple laser beam generation using diffractive masks

In the investigated methods, diffractive masks are used to generate multiple beams in desired positions and with given diameters. These masks are designed as gray-levels images to be addressed on the SLM and act as phase map objects. Each value of gray-level, different at each pixel, applies corresponding voltage and twists the liquid crystal molecules to introduce the right refractive index with direct consequence to bend properly the incident wavefront. Further, we will present two types of diffractive masks: one based on predefined number of linear blazed gratings combination LBGC and the other based on quasi-periodic structures QPSs generated using a code based on the Fourier Transform.

### 2.1. Multiple laser beam generation using combinations of linear phase gratings

In order to generate the multiple beams, we used MATHEMATICA code to calculate the diffractive masks for LBGC which are converted to phase images addressed further on the SLM (Holoeye Pluto phase-only SLM). The LBGC masks displayed on the SLM consist of a predefined number of blazed diffraction gratings with slightly different line spacing and grooves orientation relative to vertical reference, as follows:

$$G = \text{Table}[\text{Mod}[(i - 1 + \alpha * j)/d_1, 255], \{j, 1, \text{dim}G_j\}, \{i, 1, \text{dim}G_i\}] \quad (1)$$

where  $\alpha$  is the grooves orientation angle,  $d_1$  is the grooves line spacing,  $i$  and  $j$  take values between 1 and  $\text{dim}G_i$  and  $\text{dim}G_j$ , respectively; here,  $\text{dim}G_i$  and  $\text{dim}G_j$  are both equal to 300 pixels and represent the size of one blaze grating. The *Mod*

function gives the remainder on division of parameterized mask model by the grayscale value 255, while *Table* function generates a list of  $i_{max}$  copies of the involved expression.

Each blazed grating is characterized by grooves inclination angle,  $\alpha$ , relative to a vertical predefined reference (see Fig. 1 top) and the grooves spacing  $d_1$ . When a plane wave impinges one SLM addressed blazed grating mask, multiple spots are formed in the diffraction pattern. The coordinates  $(x_n, y_n)$  of the center of one spot,  $n$ , from the diffraction pattern in a plane xOy perpendicular to the propagation axis Oz depends on these parameters. From one blazed grating all spots centers are arranged collinear on a line (in a plane perpendicular to the optical axis) which forms an angle equal with  $\alpha + \pi/2$  with the same vertical reference. On this line, their distance to the optical axis is governed by the groove spacing through the grating equation,  $\sin\beta_m = m\lambda/d_1$ , where  $m$  is the diffraction order,  $\beta_m$  is the spot angle with the optical axis and  $\lambda$  is the wavelength. When many blazed gratings are implied in LBGC (Fig. 1 center), these multi-spots arrangements from individual blazed grating are formed and also some coupled terms. In this kind, more spots are obtained in a controlled manner.

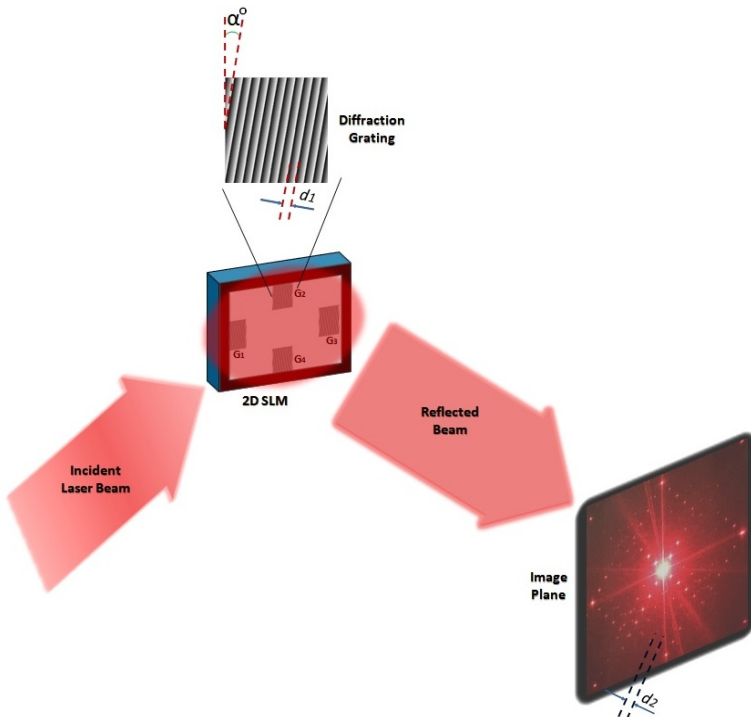


Fig. 1. Sketch of the optical setup for multiple laser beam generation employing LBGC

Figure 1 shows the design of the optical setup. The SLM is illuminated by a He-Ne laser beam with emission spectrum centered at  $\lambda=632.8$  nm, expanded

and collimated using a  $5 \times$  telescope. Once the desired parameters are established the computed grayscale LBGC masks are electronically addressed to the SLM.

The diffracted patterns are recorded as images on a high-resolution CCD camera with the pixel pitch of  $4.5 \mu\text{m}$ , positioned at a predefined distance from the SLM. With this experimental configuration, in the image plane we obtain the multiple laser spots generated in a preconfigured diffraction pattern (Fig. 1 down) according to the LBGC parameters. Therefore, the grooves orientation angle controls the line of multi-spots centers in a plane perpendicular to the propagation axis, while the different line spacing of the grooves controls the distance between spots and the propagation axis. Thus, by using this technique, the well-defined multiple spot patterns are realized with high accuracy by simple changing of the gratings parameters addressed on the SLM display.

## 2.2. Multiple laser beam generation using quasi-periodic structures

The quasi-periodic structures QPSs, like the one in Fig. 2, are generated using an algorithm based on scalar diffraction theory. It was proposed [25] based on the general idea to simulate the direct and backward propagation between two planes and then it was modified for different applications [26, 27]. Our code was implemented in MATLAB using direct and inverse bi-dimensional Fast Fourier Transform FFT to simulate the direct and backward propagation between the QPSs plane and the image plane where a desired intensity distribution is obtained.

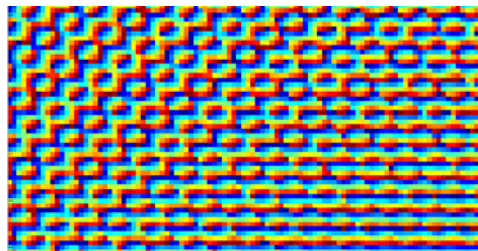


Fig. 2. Quasi-periodic structures generated using FFT as phase only diffractive masks to be addressed on SLM

The aim is to compute the transmission function in the plane of QPS that produces a desired image on the screen. Here, the desired images are formed by multiple spots characterized by established values for the radius,  $r$ , intensity and the distance,  $R$ , to the optical axis in a plane perpendicular to the optical axis situated at a given distance  $L$  along the propagation axis. The QPSs are obtained as phase only diffractive masks after few iterations of the code that reduces the distance between the desired and actual images on the screen.

Two approaches are investigated here:

1. to follow the classical algorithm based on FFT for multiple spots with the same intensity in a given plane and

2. to combine FFT in a sparse template on each depth layer, recently proposed [28]. For this, we divided the desired image of multi-spots after their depth of focalization and run the code separately for each of them; in this case, the FFT was applied in accordance with eq. (1) from [28] in its discrete form. The  $z$  parameter corresponds here with the distance along propagation axis, Oz.

The diffractive masks computed with sparse template, for each depth layer were stored and the final QPS in this case is obtained by summation of individual phase masks to experimentally evaluate the method. This approach is suitable for fast computation of phase only QPSs for multiple spots focalized in different planes perpendicular to the optical axis. Their direct application is to illuminate objects with different depths for their simultaneous monitoring.

### 3. Results and discussions

In order to generate multiple beams with a predefined distance between them ( $d_2$  = diffracted spots spacing), we studied their behavior by varying the grooves orientation angle as function of line spacing parameter. The Fig. 3 shows how the groove spacing variation influences the diffraction spots spacing in the image plane, for each of the three grooves orientation angle values ( $10^\circ$ ,  $50^\circ$  and  $80^\circ$  respectively). The smallest value considered for the groove spacing computation has been limited by the SLM display resolution and the CCD display resolution. For all three cases investigated the diffraction spots spacing presents a similar behavior showing a significant decreasing as function of groove spacing (Fig. 3). The nearly similar dependence of  $d_2$  as function of  $d_1$  proves the robustness of the method of multi spot patterns design. Thus, by simply modifying the computer grayscale LBGC parameters ( $\alpha$  and  $d_1$  for each blazed grating) we can control the diffraction spots distribution in the image plane with high accuracy.

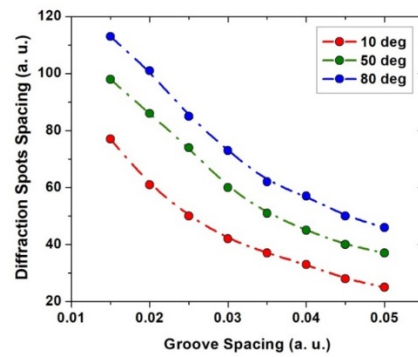


Fig. 3. Relation between groove spacing and diffraction spots spacing

In addition, to demonstrate the versatility of this method, a particular blazed grating has been computed in order to control the intensity of the multiple laser

beam spots in the image plane, but mainly for the central spot (compare Fig. 4 I and 4 II). The LBGC consists of five linear blazed gratings with no phase difference between the maximum values. The fifth grating is placed in the center of the LBGC, as shown in figure 4 II. The five gratings LBGC is addressed on the SLM following the same procedure previously described. During the image acquisition, the setup configuration remains unchanged while the two diffractive LBGSSs (Fig. 4I and 4II) succeed on the SLM display. By comparing the intensity values in the zero diffraction order, a slightly decreasing can be observed in the case of five gratings mask, while the secondary maxima remain unchanged demonstrating in this way the quantitative capability of the proposed method to influence the zero order.

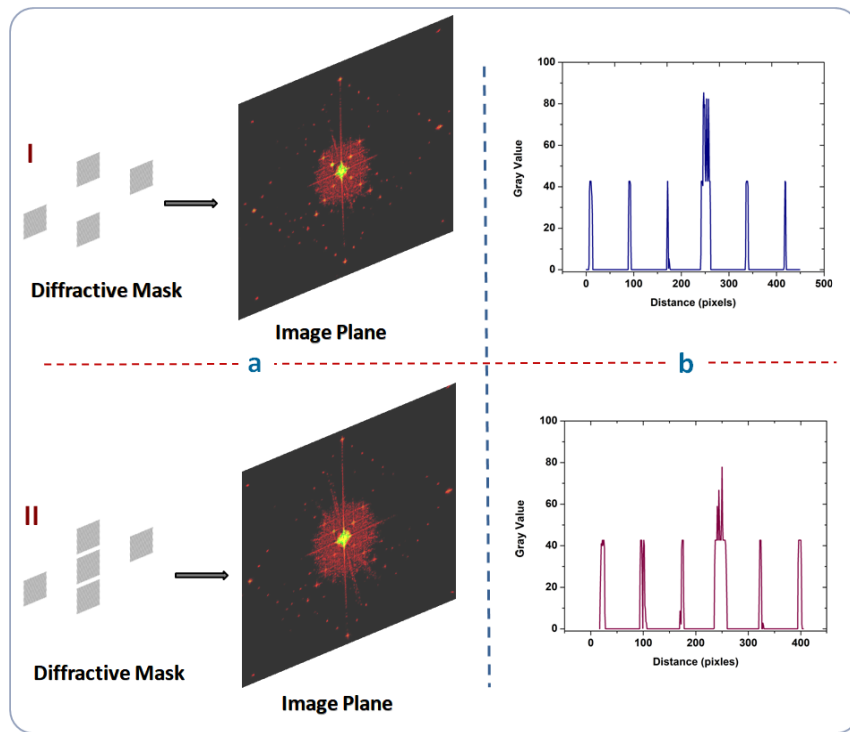


Fig. 4. a) Diffractive masks on SLM and the preconfigured diffraction patterns obtained in the image plane. b) Intensity evaluation of the multiple laser beam spots

When a QPSs is addressed on the SLM, multiple beams are generated in the far field, corresponding to first diffraction orders, equally distributed around zero order. Fig. 5 illustrates examples for two values of the spots radius,  $r$  (up and down), and four distances in a plane perpendicular to the optical axis,  $R$  (a-d). All values are normalized to the pixel pitch of the SLM.

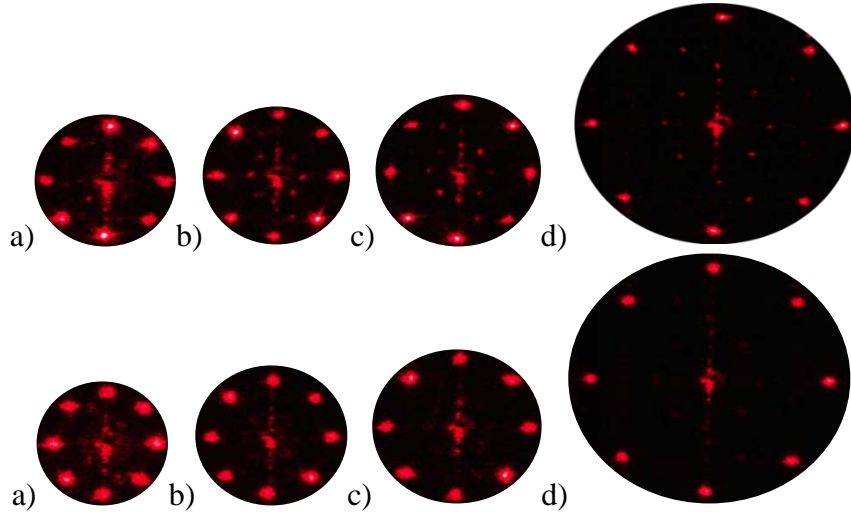


Fig. 5. Experimental diffraction patterns images obtained when QPS is addressed on the SLM, in the case of (up)  $r=2$ , (down)  $r=4$ , and a)  $R=40$ , b)  $R=50$ , c)  $R=60$ , d)  $R=120$ . Only the first order is shown for all spots.

The intensity in the diffraction pattern is measured for all investigated cases and the dependencies of the diffraction efficiency DE on  $r$  and  $R$  parameters are plotted (see Fig. 6). We computed the diffraction efficiency as the ratio between the intensity in the desired multiple-spots and the overall diffracted intensity.

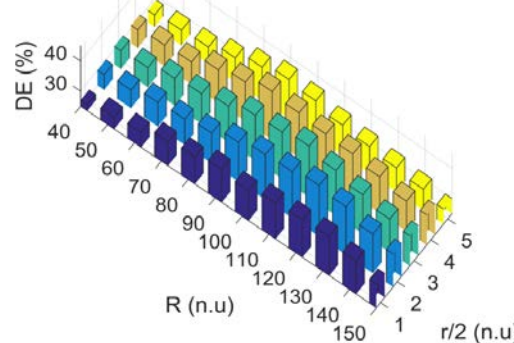


Fig. 6. Dependencies of the diffraction efficiency in the desired spots function of their radius and distance to the optical axis in a given plane perpendicular to the optical axis

All values are measured in a perpendicular plane situated at a fixed distance along the propagation axis. It is observed that for a fixed value for  $R$ , DE values increase with  $r$  up to an optimal value. This behavior is correlated with the fact that when  $r$  exceeds a critical value, the intensity is distributed on large areas and overall intensity decreases. The same behavior is observed in the case of fixed  $r$  and variable  $R$ , correlated with the fact that parasite orders appear for small  $R$ .

For diffraction patterns with multiple spots focused in different planes perpendicular to the propagation axis, we used FT in combination with sparse template to reduce the computational load. Fig. 7 comprises examples of multiple

spots in a given plane perpendicular to the optical axis in different situations: a) one spot is focused, b) three spots are focused c) all spots have the same intensity but different diameters. This method was adopted because the computational load does not increase with the number of spots, as in classical methods. In these cases, it is observed some parasite spots; the diffraction efficiency is less than in the cases of the same  $r$  and focus distance, but remains around 40%. The method allows also different  $R$  values in the same image.

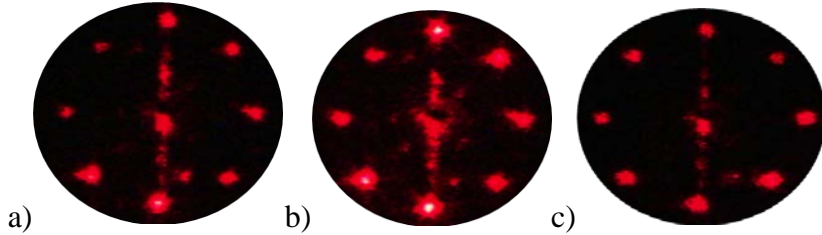


Fig. 7. Experimental diffraction patterns in a plane where a) one spot is focused, b) three spots are focused, c) all spots have equal intensity but different diameters. Only the first order is shown.

Comparing these two proposed methods for multiple-beam generation, it is noted that each one offers its own advantages. Just to mention few of them:

1. The LBGC are more simply computed. Each blazed grating is independent and it is possible to change only one of them to induce changes only in given spots. The control of multiple spots is possible with high accuracy from only two parameters: groove inclination angle and groove spacing. Using this method it is possible to control also the intensity in the zero order. By changing the computer grayscale masks parameters, it is possible to control the distribution of the laser beam spots on large areas (in the range of hundreds of square centimeters).

2. QPSs generate more efficient diffraction patterns. QPSs computed in combination with sparse template offer the possibility to have different number of focused spots in different planes along the propagation axis. In this case, **it** is possible to control each spot independently, but the computational time is greater than in the LBGC method.

3. Beside other proposals [29, 30], where all points are in the first diffraction order, grouped in one region of diffracted pattern, here, both methods (LBGC and QPS) offer the arrangement for multiple-spots on both sides of the zero order.

4. Beside [31], where all spots are symmetrically positioned around zero order and have the same intensity, here, generated QPSs allow different focus distance and diameters.

#### 4. Conclusions

Efficient methods for multi-beam array and patterns generation have been developed based on linear blazed gratings combination and on quasi-periodic structures, both displayed on a 2D spatial light modulator. These methods present

high flexibility and a precise control of the multiple laser beams parameters. The multi-spots are displayed symmetrically around the zero order and can be designed with different focus distance. Also, the methods successfully proved to offer an accurate control of the laser beam intensity in a predefined area.

These two methods for multi-spots generation were presented as alternatives to be used for simultaneous optical monitoring of different objects or several zones of the same object, but they can be used in many different applications such as micro and nano-lithography or industrial control systems (sensors, instrumentation).

### Acknowledgements

This work has been financed by the Romanian Authority for Scientific Research and Innovation, contract UEFIS-CDI, PN-III -P2-2.1-BG-2016-0288 No. 45BG/2016 and by the national projects: PNCDI III 5/5.1/ELI-RO\_2017\_16 (“SIMULATE”) under the financial support of Institute for Atomic Physics - IFA.

### R E F E R E N C E S

- [1] *Y. Ma, Y. Xia, J. Liu, S. Zhang, J. Shao, B.-R. Lu, Y. Chen*, Processing study of SU-8 pillar profiles with high aspect ratio by electron-beam lithography, *Microelectronic Engineering* **149**, 2016, pp. 141-144.
- [2] *A. Mellor, H. Hauser, C. Wellens, J. Benick, J. Eisenlohr, M. Peters, A. Guttowski, I. Tobías, A. Martí, A. Luque, B. Bläsi*, Nanoimprinted diffraction gratings for crystalline silicon solar cells: implementation, characterization and simulation, *Optics Express* **21**(S2), 2013, pp. A295-A304.
- [3] *N. Kumawat, P. Pal, M. Varma*, Diffractive Optical Analysis for Refractive Index Sensing using Transparent Phase Gratings, *Scientific Reports* **5**, 2015, pp. 16687 1-10.
- [4] *M. T. Gale, K. Knop, R. H. Morf*, Zero-order diffractive microstructures for security applications, *Proc. SPIE Optical Security and Anticount. Systems* **1210**, 1990, pp. 83-89.
- [5] *E. Lyon, Z. Kuang, H. Cheng, V. Page, T. Shenton, G. Dearden*, Multi-point laser spark generation for internal combustion engines using a spatial light modulator, *Journal of Physics D: Applied Physics*, **47**(47), 2014, pp.475501 1-8.
- [6] *S. B. Odinokov, H. R. Sagatelyan*, The Design and Manufacturing of Diffraction Optical Elements to Form a Dot-Composed Etalon Image within the Optical Systems, *Optics and Photonics Journal* **3**, 2013, pp. 102-111.
- [7] *M. Mihailescu*, Natural quasy-periodic binary structure with focusing property in near field diffraction pattern, *Optics Express* **18** (12), 2010, pp. 12526–12536.
- [8] *D. C. Dobson*, Optimal Shape Design of Blazed Diffraction Gratings, *Applied Mathematics and Optimization* **40**(1), 1999, pp. 61-78.
- [9] *Z. Kuang, D. Liu, W. Perrie, S. Edwardson, M. Sharp, E. Fearon, G. Dearden, K. Watkins*, Fast parallel diffractive multi-beam femtosecond laser surface micro-structuring, *Applied Surface Science* **255**, 2009, pp. 6582–6588.
- [10] *R. J. Beck, J. P. Parry, W. N. MacPherson, A. Waddie, N. J. Weston, J. D. Shephard, D. P. Hand*, Application of cooled spatial light modulator for high power nanosecond laser micromachining, *Optics Express* **18**(16), 2010, pp. 17059-17065.
- [11] *E. I. Scarlat, M. Mihailescu, A. Sobetkii*, Spatial frequency and fractal complexity in single-to-triple beam holograms, *Journal of Optoelectronics and Advanced Materials* **12**(1), 2010, pp. 105-109.
- [12] *T. Cizmar, H. I. C. Dalgarno, P. C. Ashok, F. J. Gunn-Moore, K. Dholakia*, Optical aberration compensation in a multiplexed optical trapping system, *Journal of Optics*, **13**(4), 2011, pp. 044008.

- [13] *V. Emiliani, D. Cojoc, E. Ferrari, V. Garbin, C. Durieux, M. Coppey-Moisan, E. Di Fabrizio*, Wave front engineering for microscopy of living cells, *Optics Express* **13**(5), 2005, pp. 1395–1405.
- [14] *R. J. Beck, A. J. Waddie, J. P. Parry, J. D. Shephard, M. R. Taghizadeh, D. P. Hand*, Adaptive Laser Beam Shaping for Laser Marking using Spatial light Modulator and Modified Iterative Fourier Transform Algorithm, *Physics Proc.* **12**( B), 2009, pp. 465-469.
- [15] *Y. Gaoa, D. Liua,, A Yanga, R. Tanga, J. Zhu*, Compensation for the spatial periodic modulation of the near-field beam with an improved iterative weight-based method, *Optik* **143**, 2017, pp. 59–65.
- [16] *L. Ionel, D. Ursescu, L. Neagu, M. Zamfirescu*, On-site holographic interference method for fast surface topology measurements and reconstruction, *Phys. Scr.* **90**, 2015, pp. 065502-065508.
- [17] *A. Jesacher, A. Schwaighofer, S. Fürhapter, C. Maurer, S. Bernet, M. Ritsch-Marte*, Wavefront correction of spatial light modulators using an optical vortex image, *Optics Express*, **15**(9), 2007, pp. 5801-5808.
- [18] *R. A. Banici, G. V. Cojocaru, R. G. Ungureanu, R. Dabu, D. Ursescu, H. Stiel*, Pump energy reduction for a high gain Ag X-ray laser using one long and two short pump pulses, *Optics Letters* **37** (24) 2012, pp. 5130-5132
- [19] *R. G. Ungureanu, O. V. Grigore, M. P. Dinca, G. V. Cojocaru, D. Ursescu, T. Dascalescu*, Multiple THz pulse generation with variable energy ratio and delay, *Laser Phys. Lett.* **12**, 2015 pp. 0453011-6
- [20] *M. Schneider, C. Hartwanger, H. Wolf*, Antennas for multiple spot beam satellites, *CEAS Space J* **2** 2011, pp. 59–66
- [21] *K. Naeem , I. Kwon , Y. Chung*, 2Multibeam Interferometer Using a Photonic Crystal Fiber with Two Asymmetric Cores for Torsion, Strain and Temperature Sensing, *Sensors* **17**(132) 2017, pp. 1-9
- [22] *Q. Zhou, W. Yang, F. He, R. Stoian, R. Hui, G. Cheng*, Femtosecond multi-beam interference lithography based on dynamic wavefront engineering, *Optics Express* **21** (8) 2013, pp. 9851-9861
- [23] *Y. Nakata, K. Murakawa, K. Momoo, N. Miyanaga, T. Hiromoto*, Design of interference pattern in ultra-short pulse laser processing, *Applied Physics A* **112**, 2013, pp. 191-196.
- [24] *I. Anghel, F. Jipa, A. Andrei, S. Simion, R. Dabu, A. Rizea, M. Zamfirescu*, Femtosecond laser ablation of TiO<sub>2</sub> films for two-dimensional photonic crystals, *Optics and Laser Technology* **52**, 2013, pp. 65-69.
- [25] *R. W. Gerchberg and W. O. Saxton*, A practical algorithm of the determination of the phase from image and diffraction plane pictures, *Optik* **35**, 1972, pp. 237-246
- [26] *M. Mihailescu, A. Preda, E. Scarlat, L. Preda*, Modified Gerchberg-Saxton algorithm for diffractive optical element image retrieval, *UPB Sci Bull, A*: 67(4), 2009, pp. 65-76.
- [27] *Yang, C.; Yan, H.; Wang, J.; Zhang, R.*, A novel design method for continuous-phase plate, *Optics Express*, **21**(9), 2013,11171-11180.
- [28] *Hak Gu Kim and Yong Man Ro*, "Ultrafast layer based computer-generated hologram calculation with sparse template holographic fringe pattern for 3-D object," *Optics Express* **25**, 2017, pp. 30418-30427.
- [29] *E. Lyon, Z. Kuang, H. Cheng, V. Page, T. Shenton, G. Dearden*, Multi-point laser spark generation for internal combustion engines using a spatial light modulator, *Journal of Physics D: Applied Physics* **47**, 2014, pp. 475501
- [30] *D. Engstrom, A. Frank, J. Backsten, M. Goksor, J Bengtsson*, Grid-free 3D multiple spot generation with an efficient single-plane FFT-based algorithm, *Optics Express*, **17**(12), 2009, pp. 9989-10000.
- [31] *A. Hermerschmidt, S. Krüger*, Binary diffractive beam splitters with arbitrary diffraction angles, *Optics Letters* **32**(5) 2007, pp. 448-450.